MADRID
inter.noise 2019
June 16 - 19
NOISE CONTROL FOR A BETTER ENVIRONMENT

Periodic homogenization of locally resonant uni-directionally ribbed plates

Fossat, Pascal[1]
LTDS UMR CNRS 5513, École Centrale de Lyon
36 avenue Guy de Collongue - 69134 Écully, France

Boutin, Claude[2]
LGCB-LTDS, UMR-CNRS 5513, École Nationale des Travaux Publics de l'État,
Rue Maurice Audin 69518 Vaulx-en-Velin, France

Ichchou, Mohamed [3]
LTDS UMR CNRS 5513, École Centrale de Lyon
36 avenue Guy de Collongue - 69134 Écully, France

ABSTRACT

This work deals with the dynamic behavior of periodic ribbed plates. The governing equations of the effective mechanical behavior is derived through multi-scale asymptotic homogenization method. The study focuses on situations of inner resonance that correspond to specific mechanical contrasts between the beam and plate parameters. The asymptotic homogenization process enables to upscale the local dynamics at global scale, and yields a synthetic and analytic macroscopic representation that encompasses the flexural and torsional mechanisms, as well as the unconventional dispersion features associated with inner resonance. The relevancy of homogenized models accounting for inner resonance is demonstrated using numerical computations and experimental measurements. This approach can be used to describe the motion of stiffened panels of industrial interest, design structures having specific features in a given frequency range, such as unconventional radiation efficiency and sound transmission loss.

Keywords: Homogenization, periodic structure, ribbed plate, locally resonant plate
I-INCE Classification of Subject Number: 30
(see http://i-ince.org/files/data/classification.pdf)

[1]pascal.fossat@ec-lyon.fr
[2]claude.boutin@entpe.fr
[3]mohamed.ichchou@ec-lyon.fr

1. INTRODUCTION

This paper deals with the dynamic behavior of periodic ribbed plates with inner resonance. Such structures are widely used in aeronautics where a planar structure can be stiffened by a periodic layout of beams. The common ribbed plate model given by the equivalent orthotropic plate with effective rigidities fails to describe the specific dynamic features. In dynamics, a reference study on heterogeneous uni-directionally ribbed plates has been conducted by [1] assuming that a pure flexural motion exists in the plate and a coupled flexural/torsional motion exists is the stiffner. This approach leads to analytical but implicit dispersion equations that must be solved numerically. The relevancy of these equations was validated using WFEM (Wave Finite Element Method) [2]. However, these do not provide analytical explicit expressions including the effect of local resonance involved at both micro-and macro-scales, nor understanding of the dispersion curves.

The purpose of the present work is to derive asymptotic homogenized model for a ribbed plate for which the unit cell comprises a beam clamped along a plate edge, as illustrated in figure 1. Assuming that the size of the constitutive cell is short with respect to the wavelength, the macroscopic behavior is determined by using an asymptotic homogenization method [3–5]. The derived models are subsequently used to evaluate the effective behavior of structures in which high geometrical and mechanical contrast can occur and enhanced kinematics is observed [6–9]. Section 2 presents the homogenized model, section 3 suggests a numerical validation based on WFEM computations, and section 4 compares the proposed model with experimental measurements.

2. OVERVIEW OF THE 1D-RIBBED PLATE MODEL

This part summarizes the uni-directionally plate model presented in [9] and shortly presents its results. Such a review introduces the key points to derive the ribbed plate model based on the physical insight, briefly presents the guidelines for the homogenization process, and sets out arguments for the coupling step. The final model consists in a set of equations associated with the flexural (2.1), torsional (2.2), and guided waves (2.3).

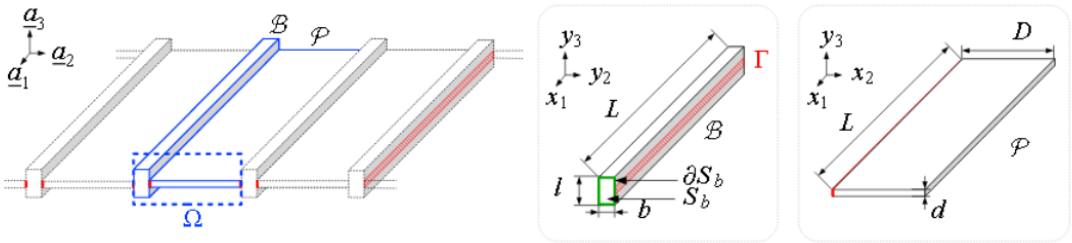

Figure 1: Periodic 1D-ribbed plate with constitutive cell Ω *and coordinates associated with the beam* $\mathcal{B}$ *and the plate* $\mathcal{P}$ *clamped on their interfaces* Γ.

The asymptotic method is used to obtain the effective macroscopic governing equations through the derivation of the beam and plate models. The model will be derived in the scope of non-homogeneous kinematics since it is considered that the beam imposes its displacement to the plate. This derivation considers first the case of a beam with an unknown load on the junction. The plate model is then obtained and enables to identify the in-plane and out-of-plane stresses that will be balanced by the unknown

stresses in the beam. The full coupling is achieved for bending and torsional behavior.

2.1. Homogenized formulation of the flexural behavior of ribbed plates

The purpose of the present example is to sum up the homogenized model for a ribbed plate. Assuming that the size of the constitutive cell is short with respect to the wavelength, the macroscopic behavior is determined by homogenization.

Asymptotic model of transversely loaded beam : the beam is considered to be straight and homogeneous and the slenderness criterion is satisfied for $\epsilon_b = l/L << 1$. Let us introduce the macroscopic variable x_1 along the axial direction and two microscopic variables $y_\alpha = \epsilon_b^{-1} x_\alpha$, with $\alpha = 2, 3$ along the section plane directions. The reference frame associated with coordinates (x_1, y_2, y_3) is $(\underline{a}_1, \underline{a}_2, \underline{a}_3)$.Finally the $\underline{a}_3$-transverse vibrations of $\mathcal{B}$ are described by the following equations :

$$\begin{cases} \partial_{x_1} T^{\mathcal{B}} + \mathcal{F} = -\Lambda_b \omega^2 U(x_1) \quad \text{with } \mathcal{F} = \displaystyle\int_{\Gamma_b^+} \sigma_{23} - \int_{\Gamma_b^-} \sigma_{23} \\ \partial_{x_1} M^{\mathcal{B}} + C - T_3^{\mathcal{B}} = 0 \qquad \text{with } C = \displaystyle\int_{\Gamma_b^+} y_3 \sigma_{12} - \int_{\Gamma_b^-} y_3 \sigma_{12} \\ M^{\mathcal{B}} = -E_b I_b \partial_{x_1}^2 U(x_1) \end{cases} \tag{1}$$

The coupling with the plate consists in a shear force $\mathcal{F}$ associated with the stresses σ_{23} and a couple C related to σ_{12}.

Dynamic regime of the plate driven by the beam motion : the flatness criterion of the plate is satisfied for $\epsilon_p = d/D << 1$. In this case, two macroscopic variables x_α with $\alpha = 1, 2$ and the microscopic variable $y_3 = \epsilon_p^{-1} x_3$, are used to describe the system.The transverse displacement w of $\mathcal{P}$ is then governed by the classical Kirchhoff equation.

However, the condition of scale separation means that the wavelength along L is much larger than that along D, then the displacement variation $\partial_{x_1} w \ll \partial_{x_2} w$. In the plate $\mathcal{P}$, the derivatives with respect to x_1 are negligible compared to derivatives with respect to x_2. Consequently, the 2D plate equation reduces to a 1D equation Equation 2 involving x_2 only :

$$\begin{cases} \partial_{x_2} T^{\mathcal{P}} = -\Lambda_p \omega^2 w; \qquad \partial_{x_2} M^{\mathcal{P}} - T^{\mathcal{P}} = 0; \qquad M^{\mathcal{P}} = -E'_p I_p \partial_{x_2}^2 w & \text{in } \mathcal{P} \\ \forall x_1 : \qquad w(x_1, x_{2|\Gamma}) = U(x_1); \qquad \partial_{x_2} w(x_1, x_{2|\Gamma}) = 0; & \text{on } \Gamma_p \end{cases} \tag{2}$$

By continuity, the beam and the plate displacements are identical at their interfaces, i.e., $w_{\Gamma_p^-} = U_{\Gamma_b^+}$, and, by periodicity, $w_{\Gamma_p^+} = U_{\Gamma_b^-}$. In addition, a clamped condition applies on the plate extremities, i.e. $\partial_{x_2} w(x_1, x_{2|\Gamma_p}) = 0$. It results that the set Equation 2 is a linear problem where the displacement $U(x_1)$ is the forcing term. Thus, $w(x_1, x_2)$ takes the form $w(x_1, x_2) = U(x_1)\phi_\omega(x_2)$ where $\phi_\omega(x_2)$ is the frequency dependent solution of the classical one-dimensional harmonic bending equation here below in which appears the natural flexural wavenumber $\delta^4 = \Lambda_p \omega^2 / (E'_p I_p)$. The resolution of Equation 2 is straightforward and reads its solution :

$$\phi_\omega(x_2) = \frac{\cosh(\delta x_2)\sin(\delta^*) + \cos(\delta x_2)\sinh(\delta^*)}{\cosh(\delta^*)\sin(\delta^*) + \cos(\delta^*)\sinh(\delta^*)}; \quad -D/2 < x_2 < D/2; \quad \delta^* = \frac{\delta D}{2} \tag{3}$$

The expression of $\phi_\omega(x_2)$ highlights the resonant nature of the plate response at the specific frequencies corresponding to the odd modes of the plate. The anti-symmetric modes of the clamped plate do not participate to the forced motion ϕ_ω.

Beam/plate coupling : the coupling terms involved in the beam balance Equation 1 are given by the displacement field in the plate. The couple arising from σ_{p12} vanishes due to clamped condition Γ_p, then $C = 0$. Expressing the beam/plate stress continuity at their interface and accounting for the periodicity we have $\sigma_{T12|\Gamma_b^\mp} = \sigma_{p12|\Gamma_p^\pm} = 0$ and $\sigma_{S23|\Gamma_b^\mp} = \sigma_{t23|\Gamma_p^\pm}$. Then, using the plate equation Equation 2, the force exerted by the plate on the beam (see Equation 1) reads

$$\mathcal{F} = T^{\mathcal{P}}_{|\Gamma_p^-} - T^{\mathcal{P}}_{|\Gamma_p^+} = -\int_{-D/2}^{D/2} \partial_{x_2} T^{\mathcal{P}} \mathrm{d}x_2 = \Lambda_p \omega^2 \int_{-D/2}^{D/2} W \mathrm{d}x_2 = \Lambda_p D \langle \phi_\omega \rangle \omega^2 U(x_1) \quad (4)$$

The above results Equation 4 show that the plate exerts a shear force in the form of a inertial term with a non-conventional frequency dependence arising from $\langle \phi_\omega \rangle$. This expression reported in Equation 1 provides the effective modeling of the ribbed plates in bending Equation 5. This formulation encompasses the global modes associated with the flexural inertia of the beam and a non conventional effective beam/plate inertia that includes the frequency dependent effective mass of the plate in dynamic regime :

$$\begin{cases} \partial_{x_1} T^{\mathcal{B}} + \omega^2 \Lambda_p D \langle \phi_\omega \rangle U(x_1) = -\omega^2 \Lambda_b U(x_1) \\ \partial_{x_1} M^{\mathcal{B}} - T_3^{\mathcal{B}} = 0 \qquad \text{with } \langle \phi_\omega \rangle = \dfrac{1}{D} \displaystyle\int_{-D/2}^{D/2} \phi_\omega(x_2) \mathrm{d}x_2 = \dfrac{2}{\delta^*} \dfrac{1}{\coth(\delta^*) + \cot(\delta^*)} \\ M^{\mathcal{B}} = -E_b I_b \partial^2_{x_1} U(x_1) \end{cases} \quad (5)$$

2.2. Homogenized formulation of the torsional behavior of ribbed plates :

The analysis in torsion is performed assuming that the beam $\mathcal{B}$ is loaded in torsion :

$$\begin{cases} \partial_{x_1} \mathcal{M}^{\mathcal{B}} + \mathcal{T} = -\omega^2 \rho_b J_b \theta(x_1) \qquad \text{with } \mathcal{T} = \displaystyle\int_{\Gamma_b} y_2 \sigma_{32}.n_2 - \int_{\Gamma_b} y_3 \sigma_{22}.n_2 \\ \mathcal{M}^{\mathcal{B}} = G_b \mathcal{I}_b \partial_{x_1} \theta(x_1) \end{cases} \quad (6)$$

where the torque $\mathcal{T}$ accounts for the action of the plate on the beam.The plate $\mathcal{P}$ in bending is described by the set Equation 2. Assuming scale separation, the description reduces to Equation 7 except for the boundary conditions. Here the proper boundary conditions express that Γ_b^- and Γ_b^+ follows the same rotation $\theta(x_1)$,thus, the plate problem reads now

$$\begin{cases} \partial_{x_2} T^{\mathcal{P}} = -\Lambda_p \omega^2 w; \qquad \partial_{x_2} M^{\mathcal{P}} - T^{\mathcal{P}} = 0; \qquad M^{\mathcal{P}} = -E'_p I_p \partial^2_{x_2} W & \text{in } \mathcal{P} \\ \forall x_1 : \qquad w(x_1, x_{2|\Gamma}) = 0; \qquad \partial_{x_2} w(x_1, x_{2|\Gamma}) = \theta(x_1); & \text{on } \Gamma_p \end{cases} \quad (7)$$

The solution of this linear problem in which rotation $\theta(x_1)$ is the forcing term takes the form $W(x_1, x_2) = D\theta(x_1)\psi(x_2)$ where $\psi_\omega(x_2)$ is the frequency dependent solution of $\partial^4_{x_2}\psi_\omega - \delta^4 \psi_\omega = 0$ with $\psi_\omega(x_{2|\Gamma_p}) = 0$ and $\partial_{x_2}\psi_\omega(x_{2|\Gamma_p}) = 1/D$. The resolution provides

$$\psi_\omega(x_2) = \frac{\sinh(\delta x_2)\sin(\delta^*) - \sin(\delta x_2)\sinh(\delta^*)}{2\delta^*(\cosh(\delta^*)\sin(\delta^*) - \cos(\delta^*)\sinh(\delta^*))} \quad ; \quad -D/2 < x_2 < D/2 \quad (8)$$

The denominator of $\psi_\omega(x_2)$ vanishes for the eigenfrequencies of the anti-symmetric modes of the plate. The beam/plate coupling through the torque $\mathcal{T}$ is derived from the stress continuity and the periodicity that provides $\sigma_{22|\Gamma_b^\mp} = \sigma_{22|\Gamma_p^\pm}$ and $\sigma_{23|\Gamma_b^\mp} = \sigma_{23|\Gamma_p^\pm}$. Then the action of the plate on the beam in Equation 6 reads :

$$\mathcal{T} = \frac{b}{2}\left(T^{\mathcal{P}}_{|\Gamma_p^-} + T^{\mathcal{P}}_{|\Gamma_p^+}\right) - M^{\mathcal{P}}_{|\Gamma_p^-} + M^{\mathcal{P}}_{|\Gamma_p^+} \tag{9}$$

Now, from the plate equation 7 we have on the one hand

$$M^{\mathcal{P}}_{|\Gamma_p^+} - M^{\mathcal{P}}_{|\Gamma_p^-} = \frac{D}{2}(T^{\mathcal{P}}_{|\Gamma_p^+} + T^{\mathcal{P}}_{|\Gamma_p^-})| + \Lambda_p D^3 \langle \frac{x_2}{D}\psi_\omega \rangle \omega^2 \theta(x_1) \tag{10}$$

and on the other hand : $T^{\mathcal{P}}_{|\Gamma_p^+} = T^{\mathcal{P}}_{|\Gamma_p^-} = -E'_p I_p \partial^3_{x_2}\psi_{\omega|\frac{D}{2}} D\theta(x_1)$. Substituting the previous expressions in Equation 6 provides the effective torsional modeling Equation 11, Equation 12, Equation 13. This formulation includes the global modes associated with the non conventional effective beam/plate rotational inertia, that contains *i)* the static rotational inertia of the beam and the effective rotational inertia of the plate J^*_ω - and *ii)* a frequency dependent torsional spring rigidity C^*_ω :

$$\begin{cases} \partial_{x_1}\mathcal{M}^{\mathcal{B}} + \omega^2 \Lambda_p D^3 J^*_\omega \theta(x_1) - \dfrac{E'_p I_p (D+b)}{D^2} C^*_\omega \theta(x_1) = -\omega^2 \rho_b J_b \theta(x_1) \\ \mathcal{M}^{\mathcal{B}} = G_b \mathcal{I}_b \partial_{x_1}\theta(x_1) \end{cases} \tag{11}$$

with

$$J^*_\omega = \langle \frac{x_2}{D}\psi_\omega \rangle = \frac{1}{D}\int_{-D/2}^{D/2} \frac{x_2}{D}\psi_\omega(x_2)\mathrm{d}x_2 = \frac{1}{(2\delta^*)^2}\frac{\coth(\delta^*) + \cot(\delta^*) - 2/\delta^*}{\coth(\delta^*) - \cot(\delta^*)} \tag{12}$$

$$C^*_\omega = D^3 \partial^3_{x_2}\psi_{\omega|\frac{D}{2}} = (2\delta^*)^2 \ \frac{\coth(\delta^*) + \cot(\delta^*)}{\coth(\delta^*) - \cot(\delta^*)} \tag{13}$$

2.3. Guided modes

The kinematics described in previous sections 2.1 and 2.2 correspond to situations where the plate is driven by the moving beams. However a second mechanism when the beams are at rest ($U(x_1) = 0$ in Equation 2 and $\theta(x_1) = 0$ in Equation 7) is associated with guided waves. At the leading order, the plate reduces to the 1D problem (similar to Equation 2 except for the zero boundary condition for ψ). Let us seek for an approximated solution in the form of separated variables :

$$w(x_1, x_2) = \exp(ik'_\omega x_1)\Psi(x_2) \qquad \text{where} \qquad \Psi(x_{2|\Gamma_p}) = 0 \quad ; \quad \partial_{x_2}\Psi(x_{2|\Gamma_p}) = 0$$

The function $\Psi(x_2)$ fluctuates according to the plate width D, while $\exp(ik'_\omega x_1)$ varies according to $L \gg D$. Consequently, at the leading order, the plate equation reduces to the following 1D-problem (identical to Equation 2 except for the zero boundary condition for Ψ):

$$E'_p I_p \partial^4_{x_2}\Psi = \Lambda_p \omega^2 \Psi \qquad \Psi(x_{2|\Gamma_p}) = 0 \quad ; \quad \partial_{x_2}\Psi(x_{2|\Gamma_p}) = 0$$

The x_1-wavenumber can then be determined by reporting the expression of $w(x_1, x_2)$, in the bilaplacian equation governing the plate $\mathcal{P}$. For each eigenmode Ψ^I, and remarking that $E'_p I_p \partial^4_{x_2}\Psi^I = \Lambda_p \omega_I^2 \Psi^I$, one obtains :

$$E'_p I_p \left[(k'^I_\omega)^4 \Psi^I - 2(k'^I_\omega)^2 \partial^2_{x_2}\Psi^I\right] = \Lambda_p(\omega^2 - \omega_I^2)\Psi^I \tag{14}$$

Hence, at frequencies lower than ω_I, the wavenumbers are complex valued or purely imaginary which corresponds to propagative damped waves or evanescent waves. Finally for frequencies higher than the clamped plate eigenfrequencies ω_I, a real positive root exists and the wave propagates without damping. Note also that these guided waves are alternatively associated with symmetric and anti-symmetric modes of the clamped plate.

3. NUMERICAL VALIDATION

The cell is modeled through a 3D finite element model. The implementation of the eigen-value problem is performed using the WFEM [2]. The numerical model captures all the mechanisms (shear, longitudinal, torsional, and flexural waves) existing in the structure, and the resulting dispersion diagram shows different branches (Fig. 2).

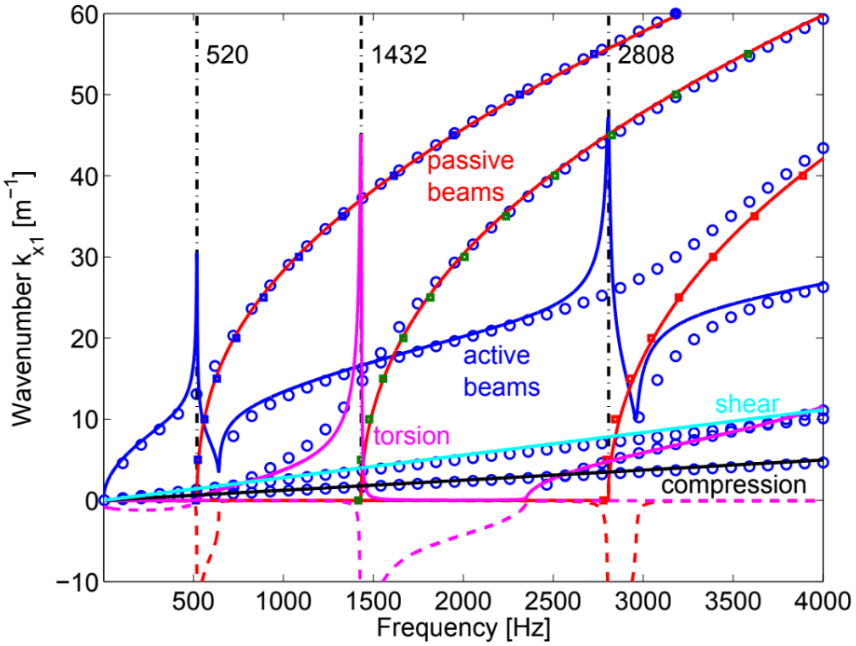

Figure 2: Dispersion curves associated with the unidirectionally ribbed plate. WFEM computation (∘), analytical homogenized model : flexural guided waves in the plate (−), flexural (−), torsional (−), longitudinal (−) and shear waves (−) in the stiffner

Figure 2 compares the proposed homogenized model with the WFEM computation. One notices a good agreement between the numerical simulation and the wavenumbers predicted by the homogenized model. The proposed model eases the understanding of the dispersion diagram. The flexural and torsional kinematics are identified. The cut-on frequencies of the guided modes are correctly estimated, as well as the the activation of torsional kinematics.

The flexural wave in the beam is affected by the effective mass of the internal resonating plate, and singularities associated with symmetric modes appear. Significant unconventional dispersion arises around the symmetric modes of the plate. In these frequency bands corresponding to negative effective mass, the flexural wave is strongly attenuated. The torsional waves are affected by the effective rotational inertia and effective spring rigidity of the internal resonating plate, and singularities corresponding to anti-symmetric modes appear. In frequency bands where the effective rotational inertia and torsional spring rigidity strongly fluctuate, the torsional waves are either evanescent

or damped. The reader may refer to [9] for a detailed analysis of these atypical dispersion features.

4. EXPERIMENTS ON UNI-DIRECTIONALLY RIBBED PLATE

This section is devoted to experiments performed on uni-directionally ribbed panel.

4.1. Investigated structure and instrumentation

The uni-directionnaly ribbed plate under study is described below and depicted in Fig. 3. Both the plate and the ribs are made of aluminium. The plate ($750 \times 600 \times 1$ mm) is ribbed with 8 stiffeners ($600 \times 10 \times 5$ mm) spaced from 90 mm.

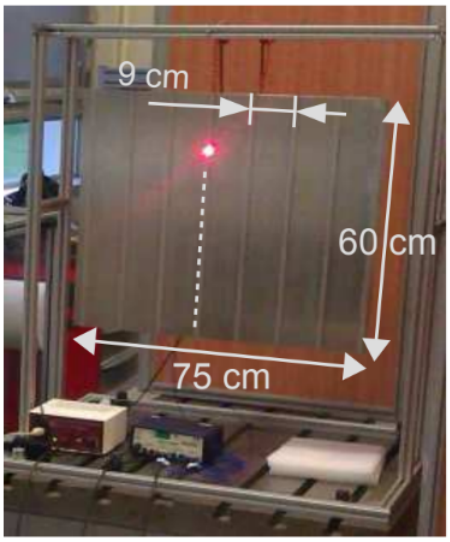

Figure 3: Uni-directionally ribbed plate under study

Experimental setup : the structure is freely suspended and excited by a shaker with a random noise in the frequency range 0-2kHz. The excitation point is located on the central stiffener. An impedance head screwed on the shaker's output gives the input force and acceleration. The velocity field is measured by a scanning vibrometer. The scan is performed on a line along the excited stiffener.

Experimental flexural dispersion curve recovery : the wavenumber extraction technique from experimental measurements is the Inhomogeneous Wave Correlation (IWC) method developed by [10, 11]. The principle is to project the experimental field on a set of inhomogeneous waves. Introducing a correlation index depending on the propagation parameters, the IWC algorithm estimates the wavenumber from the spatial field. In experimental context, the algorithm simultaneously uses the coherence function to weight the accuracy of the estimation. Identifying the maximum of this index allows to determine the propagation features. Details about outline and developments are explained in [10] and [11]. Experimental flexural dispersion curve is then recovered and compared to the analytical one.

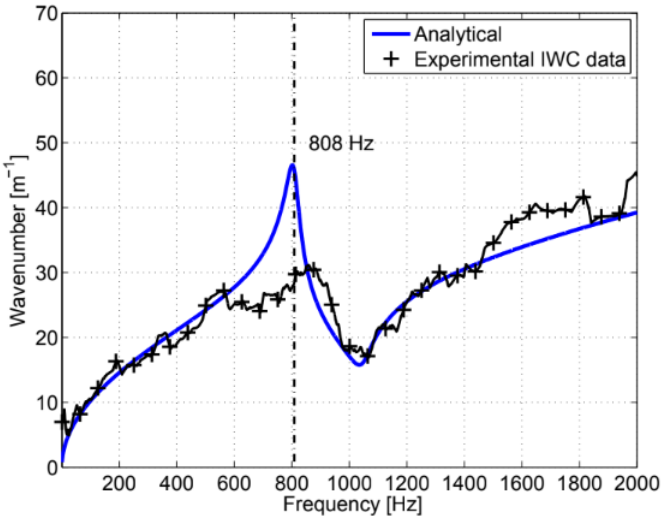

Figure 4: Flexural dispersion curves (a) analytical (−) experimental with random noise excitation signal (− + −)

4.2. Flexural wavenumber in the unidirectionally ribbed plate

Figure 4 shows the estimated dispersion curve. These measurements show that the homogenized ribbed plate model predicts correctly the wavenumber along a stiffener. The agreement with IWC is good over the whole frequency range in terms of frequency and amplitude and confirms that the experimental phenomenon is accurately captured by the homogenized ribbed plate model.

5. CONCLUSIONS

Asymptotic homogenization theory applied to a periodic ribbed plate allowed predicting its macroscopic behavior accounting for inner resonance. This model enabled to identify bending and torsion mechanisms associated with both the plate and the beam. These theoretical predictions of the wavenumbers and resonance frequencies have been successfully compared to WFEM computations. All the branches of the dispersion diagram are identified from the homogenized model. The latter captures correctly the local resonances appearing on the flexural and torsional branches as well as cut-off frequencies of the torsional and guided waves. The experimental measurements post-processed with IWC method enable to identify the flexural dispersion curve. The IWC method estimates the flexural dispersion curves from measurements. Although the IWC appears sensitive to noise, the experimental wavenumbers are in good quantitative and qualitative agreement with the theoretical predictions.

The good consistency between analytical, numerical and experimental dispersion curves demonstrates the relevance of the homogenized models to describe locally resonant uni-directionally ribbed plates.

6. ACKNOWLEDGEMENTS

This work was supported by the LabEx CeLyA (Centre Lyonnais d'Acoustique, ANR-10-LABX-0060) of Université de Lyon, within the program "Investissements d'Avenir" (ANR-11-IDEX-0007) operated by the French National Research Agency (ANR).

7. REFERENCES

[1] F.J. Fahy and E. Lindqvist. Wave propagation in damped, stiffened structures characteristic of ship construction. *Journal of Sound and Vibration*, 45(1):115 – 138, 1976.

[2] M.N. Ichchou, J. Berthaut, and M. Collet. Multi-mode wave propagation in ribbed plates. part ii: Predictions and comparisons. *International Journal of Solids and Structures*, 45(5):1196 – 1216, 2008.

[3] Enrique Sanchez-Palencia. *Non-Homogeneous Media and Vibration Theory (Lecture Notes in Physics)*. Springer, spi edition, 6 1980.

[4] C. Boutin. Microstructural effects in elastic composites. *International Journal of Solids and Structures*, 33(7):1023 – 1051, 1996.

[5] J.-L. Auriault, C. Boutin, and C. Geindreau. *Homogenization of Coupled Phenomena in Heterogenous Media (ISTE)*. Wiley-ISTE, 1 edition, 8 2009.

[6] J.-L. Auriault and G. Bonnet. Dynamique des composites élastiques périodiques. *Arch Mech.*, 37(4-5):269–284, 1985.

[7] J.-L. Auriault and C. Boutin. Long wavelength inner-resonance cut-off frequencies in elastic composite materials. *International Journal of Solids and Structures*, 49(23–24):3269 – 3281, 2012.

[8] C. Chesnais, C. Boutin, and S. Hans. Effects of the local resonance on the wave propagation in periodic frame structures: Generalized newtonian mechanics. *The Journal of the Acoustical Society of America*, 132(4):2873–2886, 2012.

[9] P. Fossat, C. Boutin, and M. Ichchou. Dynamics of periodic ribbed plates with inner resonance: Analytical homogenized model and dispersion features. *International Journal of Solids and Structures*, 152-153:85 – 103, 2018.

[10] J. Berthaut, M.N. Ichchou, and L. Jezequel. K-space identification of apparent structural behaviour. *Journal of Sound and Vibration*, 280(3–5):1125 – 1131, 2005.

[11] M.N. Ichchou, J. Berthaut, and M. Collet. Multi-mode wave propagation in ribbed plates: Part i, wavenumber-space characteristics. *International Journal of Solids and Structures*, 45(5):1179 – 1195, 2008.